Deposition and deformation of fluvial–lacustrine sediments of the Upper Triassic–Lower Jurassic Whitmore Point Member, Moenave Formation, northern Arizona

Lawrence H. Tanner [a,*], Spencer G. Lucas [b]

[a] Department of Biology, Le Moyne College, 1419 Salt Springs Road, Syracuse, New York 13214, USA
[b] New Mexico Museum of Natural History, 1801 Mountain Road, N.W., Albuquerque, New Mexico 87104, USA

ARTICLE INFO

ABSTRACT

The stratigraphic section of the Upper Triassic–Lower Jurassic Whitmore Point Member of the Moenave Formation at Potter Canyon, Arizona, comprises c. 26 m of gray to black shales and red mudstones interbedded with mainly sheet-like siltstones and sandstones. These strata represent deposition from suspension and sheetflow processes in shallow, perennial meromictic to ephemeral lakes, and on dry mudflats of the terminal floodout of the northward-flowing Moenave stream system. The lakes were small, as indicated by the lack of shoreline features and limited evidence for deltas. Changes in base level, likely forced by climate change, drove the variations between mudflat and perennial lacustrine conditions. Lenticular sandstones that occur across the outcrop face in the same stratigraphic interval in the lower part of the sequence represent the bedload fill of channels incised into a coarsening-upward lacustrine sequence following a fall in base level. These sandstones are distinctive for the common presence of over-steepened bedding, dewatering structures, and less commonly, folding. Deformation of these sandstones is interpreted as aseismic due to the lack of features typically associated with seismicity, such as fault-graded bedding, diapirs, brecciated fabrics and clastic dikes. Rapid deposition of the sands on a fluid-rich substrate produced a reverse density gradient that destabilized, and potentially fluidized the underlying, finer-grained sediments. This destabilization allowed synsedimentary subsidence of most of the channel sands, accompanied by longitudinal rotation and/or ductile deformation of the sand bodies.

© 2009 Elsevier B.V. All rights reserved.

1. Introduction

Soft-sediment deformation features are known from a wide variety of depositional environments, both terrestrial and marine, but they are particularly well-reported from lacustrine and lacustrine–deltaic depositional environments (e.g., Sims, 1973, 1975; Hesse and Reading, 1978; Seilacher, 1984; Plint, 1985; Van Loon et al., 1995; Rodrìguez Pascua et al., 2000; Rossetti and Góes, 2000; Gibert et al., 2005; Neuwerth et al., 2006; Moretti and Sabato, 2007; Singh and Jain, 2007). In most cases, however, their origins are attributed to seismic activity. One notable exception is the deformation of deltaic sandstones on a Gilbert-type delta in the (Eocene) Laney Member of the Green River Formation reported by Stanley and Surdam (1978). In particular, these authors described kidney-shaped sandstone pillows formed by the (aseismic) foundering of delta-front sands into the finer-grained prodelta muds. The authors found that the axial plane of the pillows was oriented consistently perpendicular to the paleoslope direction, with the plane inclined downslope,

although Potter and Pettijohn (1963) had discounted the value of such features as paleoslope indicators.

On the southern Colorado Plateau of southern Utah–northern Arizona, the Whitmore Point Member of the Moenave Formation has been interpreted previously as the lacustrine-dominated portion of the mosaic of terrestrial subenvironments that comprise the uppermost Triassic to Lower Jurassic Moenave Formation (Wilson, 1967; Kirkland and Milner, 2006; Tanner and Lucas, 2007, 2009). Deposition took place in ephemeral and shallow perennial lakes on the terminal floodplain, or floodout, of the Moenave stream system. This paper examines the sedimentology of the Whitmore Point Member at Potter Canyon in northern Arizona, a location that is unique (within this formation) for the presence of soft-sediment deformation features in the lacustrine sequence.

2. Regional setting

During the Early Mesozoic (Late Triassic through Early Jurassic) the Colorado Plateau was located at near-equatorial latitudes (5° to 15° N) (Scotese, 1994; Molina-Garza et al., 1995, Kent and Olsen, 1997) within a retro-arc basin on the western edge of the North American craton. The basin, the continental portion of which extended from southwestern Texas to northern Wyoming, formed

as a consequence of the initial growth of the Cordilleran magmatic arc (Dickinson, 1981; Lucas et al., 1997). Deposition of the Moenave Formation took place during the Late Triassic to Early Jurassic across a broad, low-gradient alluvial plain (Blakey and Gubitosa, 1983; Clemmensen et al., 1989; Tanner and Lucas, 2007, 2009). Sedimentation was controlled primarily by streams flowing north to northwest from highland source areas located approximately 500 km to the south and southwest, and (to a lesser extent) 200 to 300 km to the east and northeast (Blakey and Gubitosa, 1983; Marzolf, 1994).

Basal Moenave strata were deposited unconformably on the mainly alluvial strata of the Upper Triassic (Carnian to Rhaetian) Chinle Group following an interval of lowered base level and incision that may have coincided with tectonic reorganization of the basin and fore-bulge migration (Tanner, 2003a). The unconformity that separates basal Moenave strata from the Owl Rock Formation of the Chinle Group has been termed the J-0 unconformity and classically has been considered to coincide with the Triassic–Jurassic boundary (e.g., Pipiringos and O'Sullivan, 1978). However, as discussed by Lucas et al. (1997), Molina-Garza et al. (2003) and Tanner and Lucas (2007), this unconformity is correlative with the Tr-5 unconformity that underlies the Rock Point Formation of the Chinle Group to the east. Furthermore, as the strata both below and above this unconformity are demonstrably Triassic in age (discussed below), the term J-0 is superfluous. Uppermost strata of the Moenave Formation — of the upper Dinosaur Canyon Member and the laterally equivalent Whitmore Point Member — are overlain disconformably by the Kayenta Formation of the Glen Canyon Group. In the outcrop area of the Whitmore Point Member, the basal Kayenta Formation consists of the locally conglomeratic, medium to coarse-grained sandstones of the Springdale Sandstone Member (Lucas and Tanner, 2006).

3. Stratigraphy and age

Red beds of the Moenave Formation crop out mainly in northern Arizona and southern Utah exposed prominently in the Echo Cliffs, Ward Terrace and Vermillion Cliffs, and extend westward into easternmost Nevada (Fig. 1; Harshbarger et al., 1957; Clemmensen et al., 1989; Irby, 1996a; Lucas and Heckert, 2001; Biek et al., 2007; Tanner and Lucas, 2007). To the south and east, the Moenave Formation interfingers with the eolian dune sandstones and interdune mudstones of the Wingate Sandstone (Fig. 2), which is considered a partial correlative (Harshbarger et al., 1957; Clemmensen et al., 1989; Marzolf, 1993; Tanner and Lucas, 2007). The Moenave Formation forms the base of the Glen Canyon Group and consists of, in ascending order, the Dinosaur Canyon and Whitmore Point Members. The Dinosaur Canyon Member comprises reddish-orange to light brown siltstones and sandstones of inferred fluvial and eolian origin, in varying proportions (Harshbarger et al., 1957; Clemmensen et al., 1989; Tanner and Lucas, 2007). The Dinosaur Canyon Member overlies the calcrete-bearing mudstones of the Owl Rock Formation of the Chinle Group with pronounced unconformity over most of the Moenave outcrop belt (Lucas 1993; Lucas et al., 1997).

The Whitmore Point Member was established by Wilson (1967) to differentiate the purple and gray laminated mudstones and shales in the upper part of the Moenave Formation from the orange to red sandstones and mudstones of the underlying Dinosaur Canyon Member. Wilson
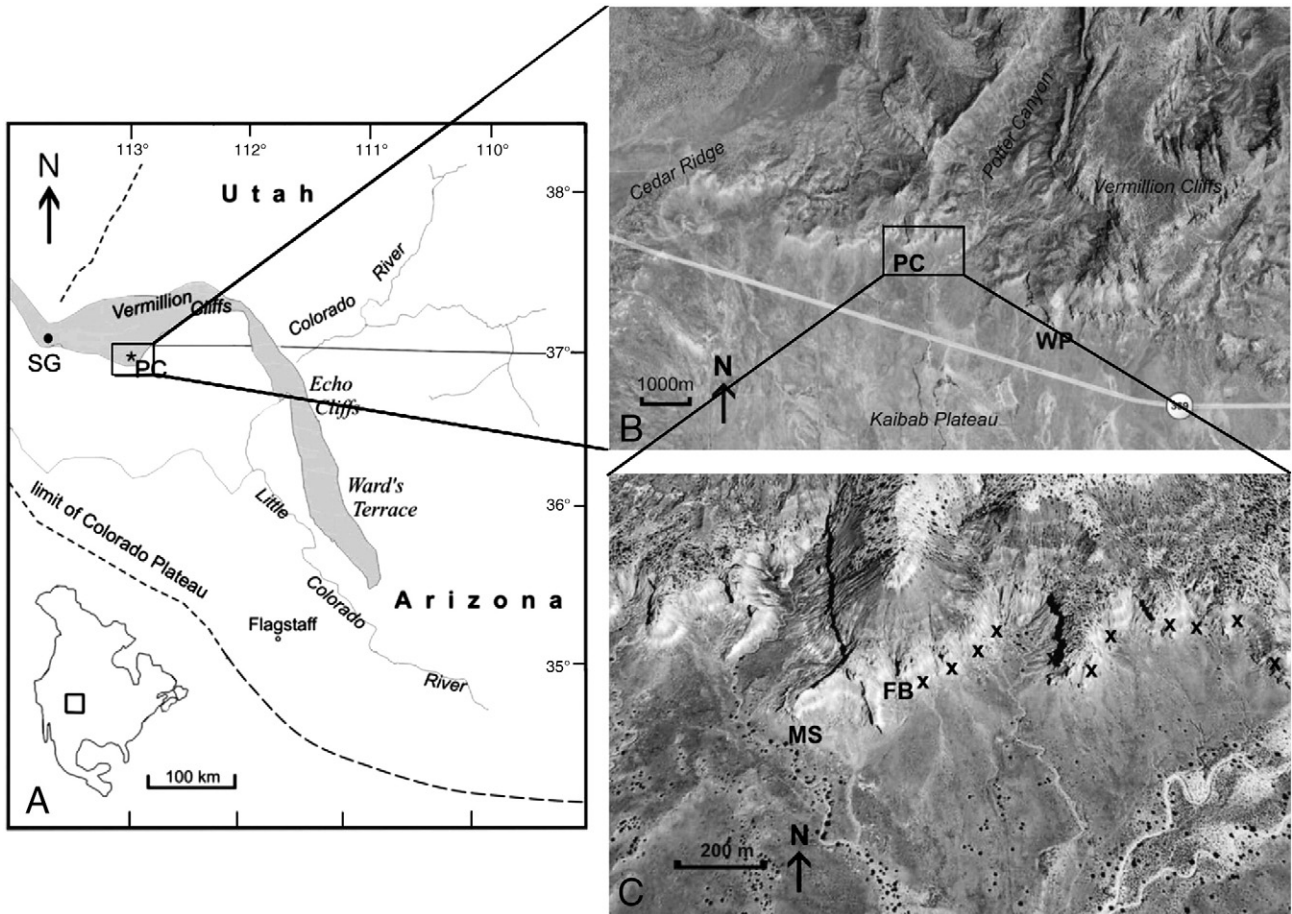
Fig. 1. Location of the study area. A) Regional setting of the study area, with outcrop limits of the Moenave Formation shaded (adapted from Tanner and Lucas, 2009). B) View of the southern flank of the Vermillion Cliffs in northernmost Arizona. PC = location of Potter Canyon section described herein. SG = St. George, Utah. WP = location of type section at Whitmore Point. C) Detail of B) showing location where section was measured (MS). FB = location of foreset bedding shown in Fig. 6. Location of individual lenticular sandstone bodies marked by x. A) adapted from Biek et al. (2007) and Tanner and Lucas (2009). B) and C) adapted from GoogleEarth®.
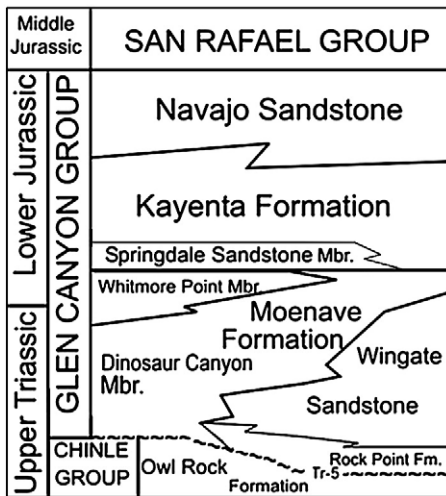
Fig. 2. General stratigraphy of the uppermost Triassic and Lower Jurassic on the Colorado Plateau.

recognized Whitmore Point strata in the northwestern part of the Moenave outcrop belt and established the type location at Whitmore Point, a south-facing promontory of the Vermillion Cliffs in Mohave County, Arizona (Fig. 1B). At the type location, the Whitmore Point Member comprises 22 m of fish- and coprolite-bearing shales, siltstones, sandstones, and minor limestones. Kirkland and Milner (2006) described the Whitmore Point Member at St. George, Utah, in considerable detail. Here, the strata form a tripartite vertical sequence comprising a lower, finer-grained unit, a middle sandy interval and an upper thin-bedded interval, recording two distinct cycles of deepening and shallowing of a lacustrine basin. The outcrops at the type location, about 73 km to the east–southeast, display a similar vertical organization.

Tanner and Lucas (2009) interpreted the Whitmore Point Member broadly as comprising the deposits of ephemeral and perennial lakes that were subject to periods of desiccation and incursions of coarse clastics during floods. They further concluded that the lakes were meromictic during perennial episodes, probably due to salinity stratification, which enhanced preservation of organic matter. These lakes formed on the non-channeled alluvial plain, or floodout (*sensu* Tooth, 2000), of a north–northwest oriented (relative to modern geography) system of mainly ephemeral streams on a broad and open floodplain. The Whitmore Point Member overlies and interfingers laterally with alluvial red-bed facies of the Dinosaur Canyon Member of the Moenave Formation (Biek, 2003a,b).

At the type location, the Whitmore Point strata are truncated by thick-bedded, cliff-forming sandstones of the Springdale Sandstone Member of the Kayenta Formation with meter-scale erosional relief (Fig. 3). However, as noted by Tanner and Lucas (2009), at this and other Whitmore Point locations, sandstones with a "Dinosaur Canyon" aspect occur between the distinctive Whitmore Point strata and the overlying Springdale Sandstone (Fig. 4), indicating that the Whitmore Point and Dinosaur Canyon Members interfinger somewhat. The distinctive facies of the Whitmore Point Member thin to the east and north of the type area, and are replaced by laterally equivalent facies of the upper Dinosaur Canyon Member.

The age of the Moenave Formation is established by a combination of vertebrate body fossils, vertebrate ichnofossils, palynomorphs, and paleomagnetic evidence (reviewed in Lucas and Tanner, 2007; Tanner and Lucas, 2007). A latest Triassic (Rhaetian) age for the lower part of the Dinosaur Canyon Member (i.e. the base of the Moenave Formation) is suggested by tetrapod trackways that are *Grallator*-dominated but lack *Eubrontes* (Morales, 1996; Lucas et al., 1997, 2005), and by magnetostratigraphic correlation to the Newark basin section (Molina-Garza et al., 2003). A Hettangian (Early Jurassic) age for the upper Dinosaur Canyon Member (and the correlative Wingate Sandstone) is suggested by tracks of the dinosaur ichnotaxa *Eubrontes* and *Otozoum* and fossils of the crocodylomorph *Protosuchus* (Irby 1996b; Lucas and Heckert, 2001, Lucas et al., 2005). An Early Jurassic (likely Hettangian) age for at least the upper Whitmore Point Member is suggested by a *Corollina* spp. dominated palynoflora (Peterson and Pipiringos, 1979; Litwin, 1986; Cornet and Waanders, 2006) and by the lateral equivalence of the Whitmore Point Member with the upper Dinosaur Canyon Member. More recent palynological and paleomagnetic data now indicate that the lower part of the Whitmore Point Member is latest Triassic in age (Donohoo-Hurley et al., 2009). Thus, the Triassic–Jurassic boundary occurs within the Whitmore Point Member, in the upper part of the Moenave Formation.
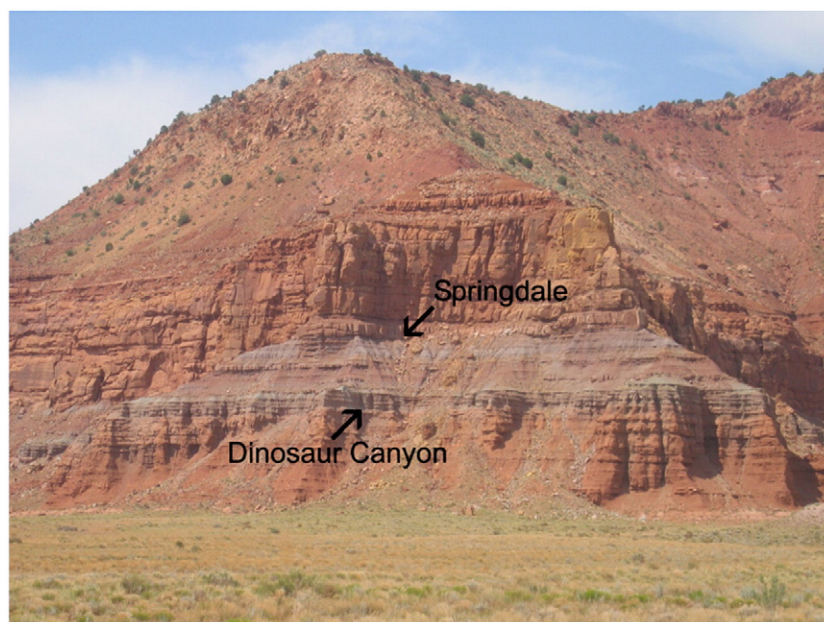
Fig. 3. View of the outcrop section measured at Potter Canyon (Fig. 4). Top of the Dinosaur Canyon Member (= base of Whitmore Point) and base of Springdale Sandstone (= top of Whitmore Point) shown. The section was measured at the right end of the outcrop shown. Thickness of the Whitmore Point section here equals c. 26 m.
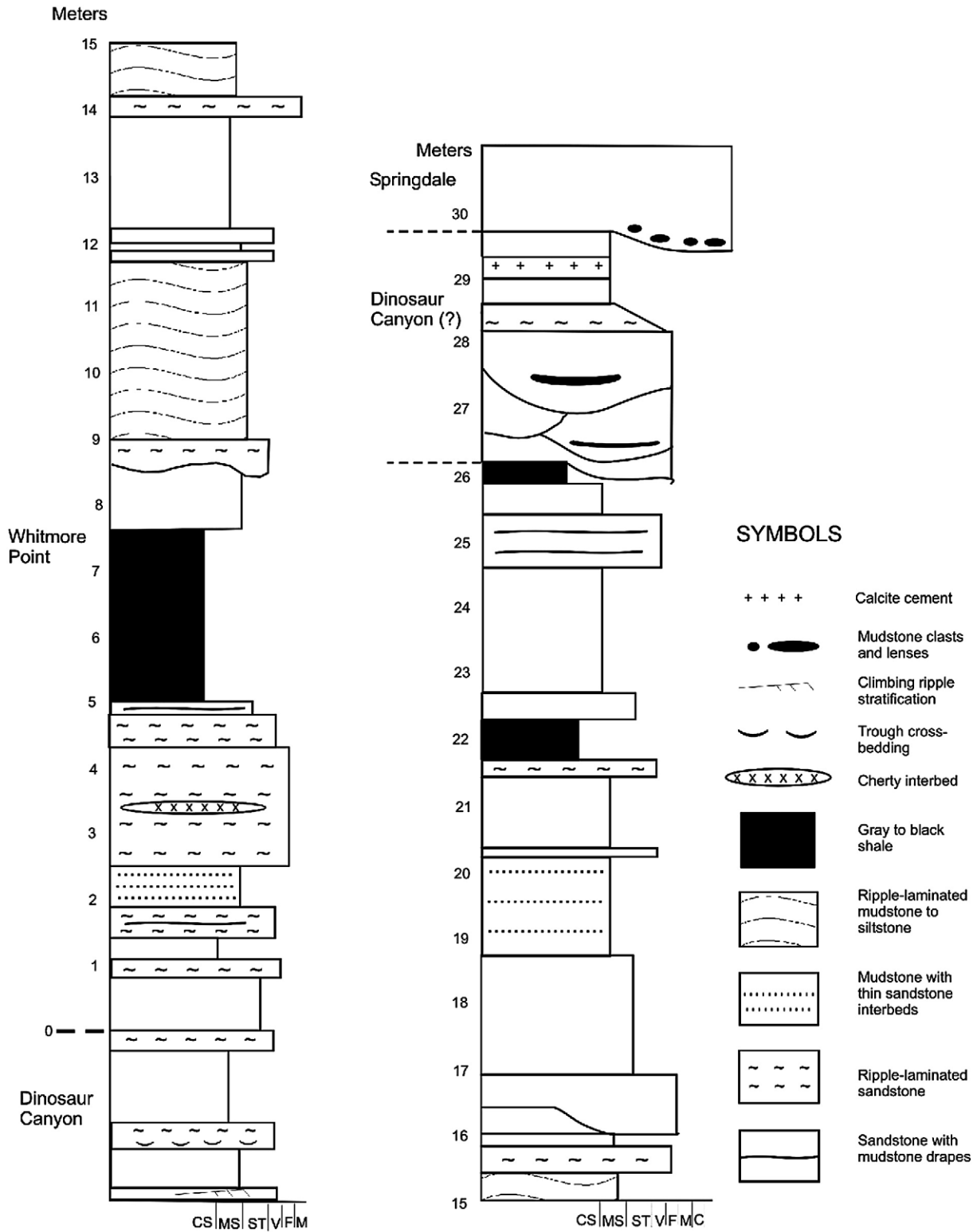
Fig. 4. Section of Whitmore Point Member of Moenave Formation section measured at location in Fig. 3. Lithologies are indicated by the grain-size scale at the base of the figure.

4. Potter Canyon section

4.1. Lithostratigraphy

This paper examines the sedimentologic features of the Whitmore Point Member on the cliffs immediately to the west of Potter Canyon, which is located to the west of Whitmore Point. Although similar lithologically to the section at the type location (at Whitmore Point),

the thickness and vertical arrangement of these facies at Potter Canyon differs somewhat. The measured section for Potter Canyon is a south-facing promontory in Mohave County in northern Arizona at 36° 52.872′ N, 112° 52.083′ W, about 3.9 km WNW of the Whitmore Point type location (Tanner and Lucas, 2009). The boundary between the Whitmore Point Member and underlying Dinosaur Canyon Member at Potter Canyon is demarcated by a distinct change in color of the rocks, from orange-reddish mudstone and very fine-

grained sandstone (of the Dinosaur Canyon Member) to grayish and purple red hues, and by an increased proportion of mudstone (in the Whitmore Point Member) (Figs. 3 and 4). Most distinctive in the Whitmore Point Member are beds of dark gray to black mudstone and shale that do not occur in the Dinosaur Canyon Member.

At Potter Canyon, the uppermost strata of the Dinosaur Canyon Member consist of red mudstones and very fine-grained sandstones displaying small-scale trough cross-beds and ripple lamination. The overlying Whitmore Point Member consists of 26.2 m of gray, purple, reddish-brown and ochre-hued shale, siltstone and sandstone (Fig. 3). The section is capped by 1.8 m of lenticular bodies of fine-grained sandstone displaying trough cross-bedding and containing discontinuous (laterally truncated) lenses of mudstone. These uppermost sandstones strongly resemble sandstones that occur in the underlying Dinosaur Canyon Member, and they contrast with the coarse-grained sandstones and intraformational conglomerates that occur immediately above. The latter we assign to the Springdale Sandstone Member of the Kayenta Formation, while the former we tentatively assign to the Dinosaur Canyon Member.

In the Whitmore Point Member, individual shale, mudstone and siltstone beds are decimeters to meters thick and exhibit lateral continuity on outcrop scale (up to hundreds of meters). Shale beds are 30 cm to 2.6 m thick, purple to black, and contain conchostracans, fish scales and coprolites. Mudstones are 20 cm to 1.7 m thick, reddish-brown to gray to purple, and commonly contain thin (cm-thick) interbedded laminae of rippled, very fine-grained sandstone or siltstone. Siltstone beds are up to 1.8 m thick, brown to gray to ochre-hued and blocky to ripple-laminated. The sandstone beds are 30 cm to 1.8 thick, but more variable in thickness than the finer-grained lithologies, with individual beds varying from meter-scale to centimeter-scale thickness, or pinching out altogether across the visible outcrop face (Fig. 5). Most sandstone beds exhibit an even, tabular geometry, but several display pronounced thickness changes over distances of a few tens of meters and have a flat-based, convex geometry (Fig. 5). Sandstone beds are typically very fine-grained and mostly display ripple lamination or horizontal lamination grading upward to ripple lamination, and in some instances, climbing ripples. Desiccation cracks, typically less than a few centimeters wide, penetrate from the bases of sandstone beds through mudstone or siltstone beds to a depth of 10 to 20 cm (Fig. 5). Lenticular sandstone bodies with meter-scale thickness but limited lateral extent occur at a single horizon at about 9.0 m above the base of the member in the measured section (Figs. 4 and 6). These sandstone bodies, most of

which display evidence of soft-sediment deformation, are described below.

The contact between the sandstones and finer-grained beds is typically sharp and non-erosive, with the exception of the lenticular sandstones described above. For the most part, sandstone beds are flat-lying and conformable with the finer-grained surrounding beds; discordance in bedding angles (beds dipping at a significant angle to regional dip) occurs in the lower part of the section (between 7.6 m and 9.0 m in the measured section), but is visible only in some outcrop faces oriented in a north to northeasterly direction. In some outcrop views, interbedded siltstone–sandstone units, 1.0 to 1.5 m thick, dip to the northeast at angles of 15° to 20° (Fig. 6). The lenticular sandstones described below occur within a single horizon immediately above these dipping beds.

Although the vertical changes in grain size between individual beds typically is very abrupt, more gradual changes among groups of beds (i.e. fining-upward and coarsening-upward sequences) are evident. For example, a pronounced fining-upward trend, from ripple-laminated sandstone to shale, is displayed between 2.5 m and 7.5 m in the measured section (Fig. 4), and again between 24.7 m and 26.2 m at the very top of the Whitmore Point Member. Only one coarsening-upward sequence is evident in the measured section; shale at 7.0 m coarsens upward to ripple-laminated sandstone at 9.0 m.

4.2. Deformed sandstones

The most unusual feature of the sedimentary section at Potter Canyon is the presence of a horizon of lenticular sandstone bodies, most displaying over-steepened, folded and/or disturbed bedding. Locations where we observed these sandstones are marked on Fig. 1C. The thickness of the sandstone bodies is variable, ranging from 2.0 m to 6.2 m, but the tops appear to share a common stratigraphic horizon. Although these sandstones are not present at the location measured for the section in Figs. 3 and 4, this horizon correlates to approximately 9 m above the base of the Whitmore Point Member, which places it above the black shale at 5.0 m to 7.6 m in the measured section and above the northeastward dipping strata in Fig. 6. The widths of the outcrop exposures of the sandstones vary from 4.4 m to 30 m. The axis of elongation of these sandstone bodies is in a general N–S direction, with the orientation of the axis for individual sandstones varying from N15°W to N40°E.

Not all of these lenticular sandstones are deformed. Fig. 7A, for example, is a view to the northwest of a 6-m thick sandstone body. Bedding within this sandstone is dominated by horizontal lamination. Most of the lenticular sandstone bodies in which bedding is preserved comprise predominantly horizontally laminated sandstone and trough cross-bedded sandstone, with sets of trough cross-beds 10 cm to 40 cm thick (Fig. 7B), and subordinate planar cross-beds.

However, most of the sandstone bodies at this stratigraphic level display some evidence of deformation, either through rotation, vertical transposition, folding, or some combination thereof. The most common style of deformation of the lenticular sandstones is longitudinal rotation, i.e., rotation of the sandstone body around an axis parallel to the direction of elongation, associated with downward movement. Fig. 8A–C are views of lenticular sandstones elongated to the northwest (outcrop orientation: north–northeast is to the right in these views). Each of these sandstones has undergone rotation with a clockwise sense (relative to the view), resulting in inclination of the bedding to the northeast. The result for the sandstones in Fig. 8A and B is the formation of a pillow shape and over-steepening of the bedding. The sandstones in Fig. 8A–D also share the characteristic that they display a fanning geometry of the bedding; i.e. the angle of inclination of the bedding decreases systematically from left to right. This effect is most pronounced in Fig. 8A and B, where the bedding on the left margin is near vertical (in Fig. 8A) to slightly overturned (in Fig. 8B),

Fig. 5. Detail of Fig. 3 illustrating general sheet-like geometry of tabular sandstones (lower) and laminated mudstones (above). Arrow indicates point of sandstone lateral pinchout and convex bedding. Desiccation cracks (dc) occur in the lower part of the section.
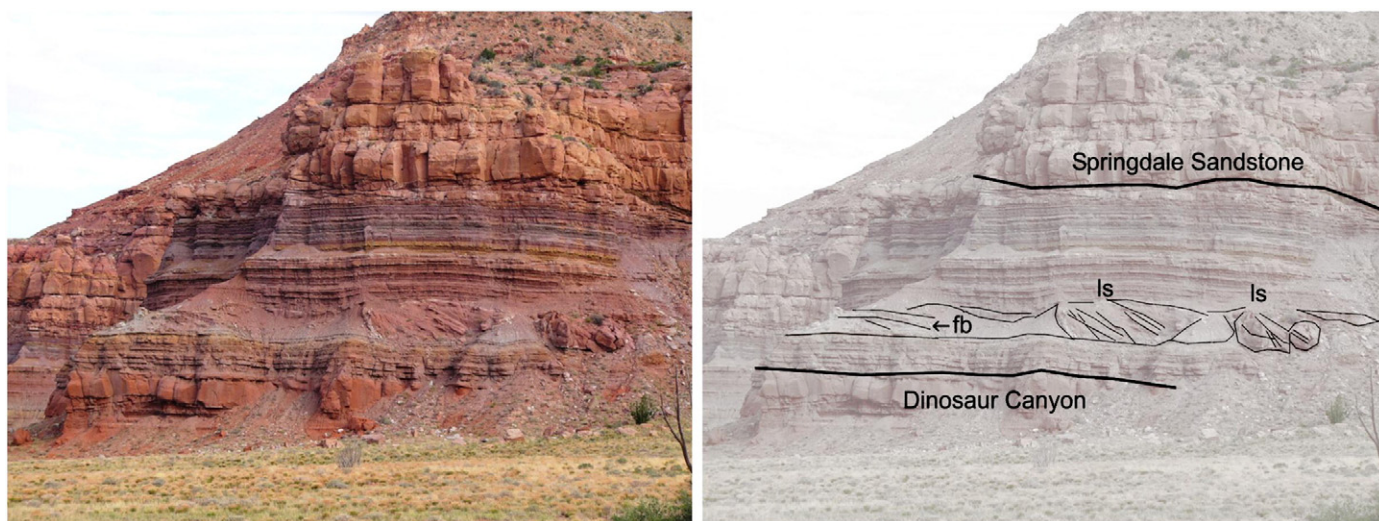
Fig. 6. View of cliff face immediately to the east of the measured section (at the location marked fb on Fig. 1C). The dipping beds to the left are interpreted as delta foreset beds (fb). Two lenticular sandstone bodies (ls) exhibiting over-steepened bedding are to the right of the dipping beds. The interpreted foresets and the lenticular sandstones occur above the lowest black shale at 5.0 m to 7.5 m in the measured section (Fig. 4).

and decreases to as little as 30° (in 8A) at the right margin. Fig. 8C demonstrates the variability of the direction of rotation; this is a view of a northeastward-oriented lenticular sandstone (south is to the right in the photograph). The bedding top is away from the viewer in this

Fig. 7. Undeformed lenticular sandstones in lower part of Whitmore Point Member. A) View of sandstone body about 6 m thick and 30 m wide that lacks features of deformation. B) Trough cross-bedding occurs at the tops of many of the lenticular sandstones (staff is 1.5 m).

example, indicating the sandstone has rotated to the northwest. In Fig. 8D, it is clear that the rotation occurred by vertical slip along a planar surface on the right (northeast) margin of the sandstone.

Over-steepened bedding (Fig. 9A–B), in which beds in the lower part of the body attain dips of 50° to 60°, is a common feature of many of the sandstones. The direction of dip appears bimodal; in some sandstones the beds dip nearly due east, as in Fig. 9A and B, but others dip nearly due west. We did not observe northerly or southerly dips, however. Notably, the over-steepened bedding is overlain in many instances by undeformed bedding, apparently disconformably. The bedding at the base of these sandstones commonly displays some degree of disruption, such as pseudoanticlines and pseudosynclines (Fig. 9C).

In some instances, the sandstone bodies display plastic deformation, or folding involving the entire body of narrow sandstones, or partial folding of wider sandstone bodies (Fig. 9D–F). Folding of narrow sandstone bodies may be expressed by simple synclinal deformation. Fig. 9D illustrates a sandstone that has folded asymmetrically; the axis of folding parallels the axis of elongation of the sandstone body (N15°E) and is inclined to the southeast, suggesting longitudinal rotation of the entire body with a northwesterly sense. This particular sandstone body also is notable for the presence of a pair of near-horizontal joint surfaces that appear unrelated to exhumation and modern slope instability. Fig. 9E and F illustrate the folding of one side of a wider sandstone body. In these figures (the view is to the north–northwest) the entire sandstone body appears rotated to the west, and the eastern margin of the sandstone (to the right in Fig. 9E) is folded to the west, as clearly illustrated in Fig. 9F. Significantly, the bedding of the strata underlying this sandstone exhibits similar deformation, wrapping around the eastern margin of the sandstone body. Many of the deformed sandstones described above also contain evidence of rapid dewatering; in particular, dewatering pipes are prominent in folded and over-steepened strata (Fig. 10A,B). These are cyclindrical features, 3 cm to 5 cm wide and 20 cm to 40 cm long, oriented perpendicular to the original bedding attitude.

5. Interpretation

5.1. Sedimentology of the Potter Canyon section

Tanner and Lucas (2007, 2009) interpreted the laterally continuous shales, mudstones and siltstones of the Whitmore Point Member

Fig. 8. Sandstone bodies in Whitmore Point Member of Moenave Formation displaying evidence of rotation. A–B) Sandstone pillows exhibiting bedding over-steepened to right (northeast) due to clockwise rotation. C) Lenticular sandstone in which direction of rotation is to the west (bedding top is away from viewer). D) The rotation of this sandstone body appears to have taken place along a planar slip surface (ss) on the right. The top of the black shale (bs) unit is visible just below the sandstone.

as the deposits of mostly shallow, ephemeral to perennial, clastic-dominated lakes of varying size. These lakes formed downstream of the Dinosaur Canyon dryland stream system on open floodplains, or floodouts (Tooth, 2000; Fisher et al., 2007; Nichols and Fisher, 2007; Tanner and Lucas, 2009). Rising base level during the late part of the interval of Moenave deposition caused partial inundation of the floodout and formed numerous broad but shallow lakes. Thus, the Whitmore Point strata were deposited on the terminal floodplain of the Moenave (Dinosaur Canyon) alluvial system, during an interval of high base level that allowed the water table to intersect the topographic surface episodically. The general correlation of the gray-black shale intervals between the Potter Canyon and Whitmore Point locations supports the interpretation that, at least locally, lake depth was controlled by changes in base level.

The Whitmore Point lakes hosted a fauna consisting primarily of abundant and diverse semionotid fish, hybodont sharks, lungfish and sizable (1 to 2 m long) coelacanths (Milner and Kirkland, 2006). The invertebrate fauna included conchostracans and various invertebrate burrowers. Shales were deposited from suspension during lake highstands in a water body with a non-vegetated bottom. The dark gray to black shale at 5.0 m to 7.6 m in the measured section indicates deposition during lake highstand in a stratified water column with dysaerobic bottom conditions that prevented aerobic decomposition or development of a benthic infaunal community. This particular bed is unique in the section for its high organic content, although other shale beds in the section are gray to grayish purple. Periodic shallowing of the lakes, culminating in evaporation and desiccation of these water bodies, is evidenced by the occurrence of sand-filled desiccation cracks at the bases of some sandstones (Fig. 5).

The middle portion of the Whitmore Point Member comprises thinly interbedded red mudstones, siltstones and sandstones. These were deposited in shallow, ephemeral lakes to dry mudflats during an interval of overall low base level. Deposition took place by unconfined sheetflow, when the mudflat was emergent, and a combination of suspension to traction currents when it was inundated. During episodes of lower base level, sheetflood events deposited tabular sheets of mostly non-graded sand across a broad alluvial mudflat (Talbot et al., 1994). On some occasions, the sheetflow produced convex-shaped bar forms on the playa (Olsen, 1989). During episodes when the mudflat was submerged, or when it became inundated during flood events, sheetflow built sheet deltas, i.e. tabular sheets of graded sand and mud that were deposited by waning flow in standing water (Smoot and Lowenstein, 1991).

The size and depth of the Whitmore Point lakes are not immediately obvious. Lateral continuity of individual beds is exhibited on the outcrop scale for tens to hundreds of meters, but does not extend to outcrops separated by several kilometers, i.e. between Potter Canyon and Whitmore Point. Therefore, we interpret the individual lakes as bodies of limited lateral extent, with surface areas that likely did not exceed several tens of km^2 to at most 100 km^2. Despite the occurrence of organic-rich facies, we interpret the lakes as shallow, even during highstands. Consequently, the abrupt changes in lithologies, e.g., gray mudstone to red mudstone or sandstone, reflect, in many instances, similarly abrupt changes between perennial and ephemeral lacustrine or playa mudflat conditions that produced no record of shoreline progradation (Bohacs et al., 2000). The single identifiable coarsening-upward sequence in the Potter Canyon section contains packages of northeast-dipping siltstone–sandstone beds that we interpret as the foresets of a small Gilbert-type delta (Fig. 6) that prograded

Fig. 9. Features of sandstone deformation. A–B) Views of sandstone bodies with over-steepened bedding overlain disconformably by undeformed trough cross-bedded sandstone (arrows). C) Disrupted bedding at base of sandstone with over-steepened bedding. Disruption consists of pseudoanticline (up arrow) and pseudosyncline (down arrow). D) Lenticular sandstone exhibiting gentle synclinal folding. Planar cross-bedding (Sp) is visible in the upper part of the sandstone, but the lower part of the unit is massive (Sm). Near-horizontal joints (js) truncate the bedding on the left side. E) Lenticular sandstone body displaying general counter-clockwise rotation and folding of the eastern flank of the body. Note that the underlying, finer-grained strata are folded parallel to the edge of the sandstone. F) Detail of folded flank of sandstone in E) illustrating the ductile behavior of the sandstone.

northeastward into the Whitmore Point lake when it was at maximum highstand, as suggested by the black shales underlying these foresets. The limited thickness of these foreset beds, however, when adjusted for sediment compaction, suggests that the water depth into which the delta prograded was on the order of 5 to 10 m.

As discussed in Tanner and Lucas (2009), neither size nor depth was a prerequisite for high organic accumulation in the Whitmore Point lakes. For example, Turcq et al. (2002) described a number of small (< 10 km²) tropical lakes in Brazil, located in a strongly seasonal climate, and found very high organic flux rates that correlated primarily with the

watershed area. Such a climate would have prevailed on the Colorado Plateau during the Late Triassic to Early Jurassic (Parrish, 1993; Tanner, 2000, 2003b; Tanner and Lucas, 2007). Small, meromictic lakes also are prone to salinity stratification, which promotes dysaerobic bottom conditions, even at shallow depth, and further enhances organic preservation, as demonstrated by Last et al. (2002). Bohacs et al. (2000) described evaporative lakes (those in underfilled basins) as characterized by thin (decimeter-scale) depositional sequences, marked by highly contrasting, laterally persistent facies boundaries, similar to the Whitmore Point facies. The Wilkins Peak Member of the
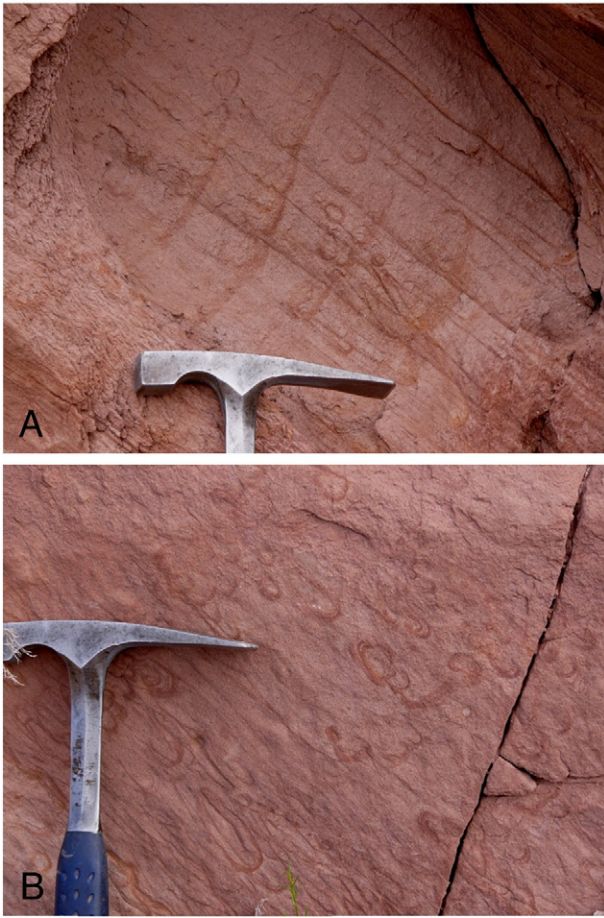
Fig. 10. Dewatering features of the deformed sandstones. A) Dewatering pipes oriented perpendicular to bedding in over-steepened sandstone. B) Oblique view of dewatering pipes in over-steepened sandstone.

(Eocene) Green River Formation provides an example of a lake in which organic productivity was promoted by the evaporatively enhanced alkalinity of the lake waters, and organic preservation facilitated by rapid burial (Bohacs et al., 2000; Pietras and Carroll, 2006).

Most of the Whitmore Point Member consists of reddish-brown to reddish-purple mudstones interbedded with decimeter-scale flat beds of reddish to ochre-hued siltstones and sandstones. The thinness of the bedding, color and the abundance of desiccation cracks in these lithologies provide ample evidence for deposition under oxidizing conditions in shallow to ephemeral water bodies with the coarser clastic sediments provided by episodes of rapid sheetflow. As these lakes formed on a broad, alluvial floodout without effective impoundment, water depth was controlled entirely by base-level change, and typically was shallow to ephemeral (Carroll and Bohacs, 1999). In this setting, the seasonal, semi-arid climate caused evaporative concentration of the water ponded in depressions on the floodout, resulting in salinity stratification of the water column and meromictic conditions. Short-term changes in base level probably reflected climatic variations, while longer-term changes (i.e. shifts between alluvial and lacustrine systems) may have resulted from eustasy, although paleogeographic reconstruction which place the study area c. 300 km from the paleoshoreline (Scotese, 1994) make eustatic controls somewhat problematic.

5.2. Lenticular sandstone bodies

The elongate geometry of the lenticular sandstones that occur about 9 m above the base of the Whitmore Point Member indicates that these were the bedload fill of alluvial channels. The bedforms within these channels (where recognizable) consist predominantly of horizontal

lamination and trough cross-bedding, and minor planar cross-bedding, which suggest that the channel-fill sedimentation was controlled mainly by flashy stream discharge, as is common in dryland river systems (Tunbridge, 1981; Sneh, 1983; Olsen, 1989; Tooth, 2000; Fisher et al., 2007). This interpretation is broadly consistent with that of Tanner and Lucas (2007) for the Dinosaur Canyon stream system. Rather than flowing across an alluvial plain, however, these channels were incised into the coarsening-upward sedimentary sequence, consisting in part of a Gilbert delta, that was deposited in the Whitmore Point lake following base-level highstand. This episode of alluvial incision likely recorded falling base level, as the overlying 10 m of strata consist entirely of reddish muds and ripple-laminated to sheet-like siltstones and sandstones, with abundant desiccation cracks. The change in base level was temporary, as highstand conditions returned later during Whitmore Point deposition, and so was likely driven by climate change (aridification). Fisher et al. (2007) remarked on the potential for climatically driven base-level changes to force cycling between lacustrine and alluvial systems within a basin.

Deformation of the channel sands appears primarily to have involved subsidence of the semi-coherent sand bodies into a soft, fluid-rich substrate. In some instances, the subsidence was contemporaneous with channel sedimentation, as indicated by the occurrence of undeformed channel sandstones that cap sandstone sequences with over-steepened bedding. Other sand bodies experienced penecontemporaneous subsidence and rotation, with rotation in the direction towards one of the channel margins. This rotation resulted from uneven subsidence of the channel; i.e. one side of the channel rotated farther than the other, causing the channel to rotate about its longitudinal axis. In several cases, the subsidence generated shear stress that caused ductile deformation of one or both of the channel margins, creating broad syncline-like folds. Concomitant deformation of the underlying, finer-grained strata from the pressure of the subsiding sand body is evidenced by folding of these strata parallel to the base of the sand body. This evidence for plasticity and the general (but not complete) lack of evidence for brittle deformation is consistent with the presence of dewatering structures. Although liquefaction did not produce grain flow in these sands, e.g. clastic dikes, it did reduce the grain-contact strength sufficiently to allow ductile behavior. These features also demonstrate that subsidence occurred before significant lithification of the sands. One exception to this is shown in Fig. 9D, where horizontal joints in the sandstone may indicate a zone of strain accommodation to the stress of folding, demonstrating partial brittle behavior of the sandstone body.

In the Whitmore Point sand bodies, there are no clear examples of flame structures, as are produced by fluidization and upward injection of the underlying sediments. For the most part, however, weathering of the finer-grained sediments that underlie and surround the sandstone bodies has obscured the nature of the bedding in these strata. In some cases, it is clear that the underlying strata were deformed in response to the loading produced by subsidence, but the true extent of fluidization of the fine-grained sediments beneath the channels is unknown. The record for the channel sands is much clearer; these experienced rapid water loss, recorded by the dewatering pipes. The preservation of bedding features and sedimentary structures in most of these sandstones demonstrates that the sands did not experience turbulence and grain flow during liquefaction, but instead remained coherent to semi-coherent. Conversely, the deformational processes associated with these sandstones did not involve significant brittle failure of bedding. Although most of the sandstone bodies display some jointing, for the most part, these appear to be either weathering-enhanced bedding surfaces or cross-cutting fractures that have been created by modern slope instability.

6. Discussion

Soft-sediment features in continental sediments commonly are attributed to seismic activity. There exists an extensive literature

devoted to the recognition of ancient seismites, with field examples ranging in age from Ordovician to Holocene (e.g., Seilacher, 1969, 1984; Vittori et al., 1991; Johnston and Schweig, 1996; Obermeier, 1996; Pope et al., 1997; Obermeier, 1998; Ettensohn et al., 2002; Merriam and Förster, 2002; Mariotti et al., 2002; Wheeler, 2002). The interpretation of seismites in the stratigraphic record typically is based on the recognition of such features as clastic dikes and sand blows (Talwani and Cox, 1985; Obermeier et al., 1990; Obermeier, 1996), formed by rapid liquefaction of buried sediment beds with a high pore pressure. Numerous other structures may be formed by seismic disturbance of sedimentary bedding; these include: fault-graded bedding, ball and pillow structures, flame structures, diapirs, wash-basin structures, boudins, and brecciated fabrics (Seilacher, 1969, 1984; Scott and Price, 1988; Dugué, 1995; Jones and Omoto, 2000; McGlaughlin and Brett, 2004). Many of these features result from thixotropic movements of destabilized, fine-grained sediment–water mixtures.

A list of criteria for recognizing seismites was presented by Sims (1975) and subsequently revised by Wheeler (2002); deformation features with a seismic origin should 1) display evidence of sudden formation, 2) display evidence of synchroneity, 3) exhibit a zoned distribution (amplitude decreasing outward), 4) exhibit an amplitude commensurate with a seismic origin, 5) occur in a tectonic setting where seismic activity is likely, and 6) occur in a depositional setting where seismic shaking is likely to cause sediment deformation. The occurrence of all of the lenticular sandstone bodies at Potter Canyon at a common stratigraphic horizon demonstrates at least approximate synchroneity of their formation (criterion 2), and the abundance of dewatering structures provides evidence of suddenness of formation (criterion 1). The extent of deformation observed at Potter Canyon is limited, however. We note that deformation in the sandstone bodies consists solely of over-steepened and rotated bedding, minor folding and water escape structures. Features of more severe deformation, such as extensively convoluted bedding, bed brecciation, microfault-ing, shear planes, clastic dikes and sand volcanoes, all commonly associated with deformation by seismic shock (Seilacher, 1969, 1984; Scott and Price, 1988; Obermeier et al., 1990; Dugué, 1995; Obermeier, 1996; Jones and Omoto, 2000; McGlaughlin and Brett, 2004; Koç Taşgin and Türkmen, 2009) are absent in this section. Additionally, the limited lateral distribution of the deformation features at Potter Canyon, combined with the total lack of deformation of some lenticular sandstones in the same horizon as those that are deformed, or of the strata adjacent to the deformed beds, suggests that these features did not result from a seismic event.

Rather, the evidence indicates that deformation was aseismic. Various aseismic mechanisms have been proposed to account for the numerous morphologies of soft-sediment deformation structures, including slope collapse, unevenly distributed surface load, deposi-tional gradient, tangential shearing and inverted density gradients (see review in Owen, 1996). Some of the Whitmore Point sandstone bodies resemble in size and shape the sandstone pillows in the Laney Member of the Green River Formation, as described by Stanley and Surdam (1978). These authors ascribed destabilization of the sediments to the depositional gradient on the front of a Gilbert-type delta. However, we find no evidence for such a depositional gradient at the horizon in which the Whitmore Point sandstone bodies occur.

Both field observations and experimentation have confirmed the importance of reverse density gradient in particular in creating gravitational instability in sediments (Blatt et al., 1972; Lowe, 1975; Allen, 1982; Owen, 1987; Selker, 1993; Owen, 1996; Rossetti, 1999; Jones and Omoto, 2000; Owen, 2003). The resultant loss of shear strength and fluidization is recorded by various types of load casts, ball and pillow structures and dewatering structures (Lowe and LoPiccolo, 1974; Lowe, 1975; Mills, 1983; Maltman, 1994; Moretti et al., 2002; Maltman and Bolton, 2003; Neuwerth et al., 2006; Koç Taşgin and Türkmen, 2009). The fluid mechanics of load cast

formation by reverse density gradients were examined by Selker (1993), who found that the simultaneous descent of the overlying denser layer and the ascent of the underlying less dense layer requires that fluidization takes place in both. Notably, this author found that only small (< 10 cm) structures are formed if Newtonian fluid properties are assumed; higher sediment–mixture viscosities result in larger load structures.

Initiation of the deformation requires some trigger that decreases sediment strength, such as an increase in pore pressure caused by loading (Jones and Omoto, 2000; Oliveira et al., 2009). Although there is a lack of direct evidence for fluidization, i.e. flame structures are not observed in the section, we conclude that deformation of the Whitmore Point channel sands was a synsedimentary response to rapid sediment loading and instability resulting from the superposi-tion of more dense sediment (sand) over less dense sediment (mud) and the consequent increase in pore pressure. Not all of the channel sands need to have subsided at exactly the same time. More likely, foundering of the channels occurred on an individual basis soon after deposition.

7. Conclusions

Detailed field observations of the Whitmore Point Member at Potter Canyon support earlier interpretations of the general sedimen-tology of these strata from other locations. The organic-rich shales, mudstones, siltstones and sandstones were deposited in shallow, perennial meromictic to ephemeral lakes and on dry mudflats on the terminal floodout of the northward-flowing Moenave stream system. The lakes were small, as indicated by the limited evidence of shoreline features and for the growth of deltas, but high productivity and possibly salinity stratification allowed preservation of organic-rich facies during highstand intervals. Changes in base level, likely forced by climate change, forced the variations between mudflat and lacustrine conditions.

Lenticular sandstones at the top of a coarsening-upward sequence represent the bedload fill of channels incised into the top of the lacustrine-fill sequence following a fall in base level. Rapid deposition of the sands produced a reverse density gradient that destabilized, and possibly fluidized, the underlying, finer-grained sediments. This destabilization caused synsedimentary subsidence of most of the channel sands, accompanied by longitudinal rotation that caused over-steepening and/or ductile deformation of the sand bodies.

References

Allen, J.R.L., 1982. Sedimentary structures: their character and physical basis. Developments in Sedimentology, vol. 30. Elsevier, Amsterdam. 663 pp.
Biek, R.F., 2003a. Geologic map of the Harrisburg Junction quadrangle, Washington County, Utah. Utah Geological Survey Map 191, 42 p., 2 plates, scale 1:24,000.
Biek, R.F., 2003b. Geologic map of the Hurricane quadrangle, Washington County, Utah. Utah Geological Survey Map 187, 61 p., 2 plates, scale 1:24,000.
Biek, R.F., Rowley, P.D., Hacker, D.B., Hayden, J.M., Willis, G.C., Hintze, L.F., Anderson, R.E., Brown, K.D., 2007. Interim geologic map of the St. George 30′ x 60′ quadrangle and east part of the Clover Mountains 30′ × 60′ quadrangle, Washington and Iron Counties, Utah: Utah Geological Survey Map, 2 plates, scale 1:100,000.
Blakey, R.C., Gubitosa, R., 1983. Late Triassic paleogeography and depositional history of the Chinle Formation, southern Utah and northern Arizona. In: Reynolds, M.W., Dolly, E.D. (Eds.), Mesozoic Paleogeography of the West- Central United States. Rocky Mountain Section SEPM, Denver, pp. 57–76.
Blatt, H., Middleton, G., Murray, R., 1972. Origin of Sedimentary Rocks. Prentice-Hall, Inc, Englewood Cliffs, New Jersey. 634 pp.
Bohacs, K.M., Carroll, A.R., Neal, J.E., Mankiewicz, P.J., 2000. Lake basin type, source potential and hydrocarbon character: an integrated sequence–stratigraphic–geochemical framework. In: Gierlowski-Kordesch, E.H., Kelts, K.R. (Eds.), Lake

Basins Through Space and Time: American Association of Petroleum Geologists Studies in Geology, vol. 46, pp. 3–34.

Carroll, A.R., Bohacs, K.M., 1999. Stratigraphic classification of ancient lakes; balancing tectonics and climatic controls. Geology 27, 99–102.

Clemmensen, L.R., Olsen, H., Blakey, R.L., 1989. Erg-margin deposits in the Lower Jurassic Moenave Formation and Wingate Sandstone, southern Utah. Geological Society of America Bulletin 101, 759–773.

Cornet, B., Waanders, G., 2006. Palynomorphs indicate Hettangian (Early Jurassic) age for the middle Whitmore Point Member of the Moenave Formation, Utah and Arizona. New Mexico Museum of Natural History and Science Bulletin 37, 390–406.

Dickinson, W.R., 1981. Plate tectonic evolution of the southern Cordillera. Arizona Geological Society Digest 14, 113–135.

Donohoo-Hurley, L.L., Geissman, J.W., Lucas, S.G., Kuerschner, W., 2009. The Triassic/Jurassic boundary, Colorado Plateau area, USA: magnetostratigraphic correlation of the Moenave Formation with the strata from the St. Audrie's Bay, UK, Morocco, and Newark/Hartford basins. Geological Society of America Abstracts with Programs 41 (7), 182.

Dugué, O., 1995. Séismites dans le Jurassique supérieur du Bassin anglo-parisien (Normandie, Oxfordien supérieur, Calcaire gréseux de Hennequeville). Sedimentary Geology 99, 73–93.

Ettensohn, F.R., Kulp, M.A., Rast, N., 2002. Interpreting ancient marine seismites and apparent epicentral areas for paleo-earthquakes, Middle Ordovician Lexington Limestone, central Kentucky. In: Ettensohn, F.R., Rast, N., Brett, C.E. (Eds.), Ancient Seismites: Geological Society of America Special Paper, vol. 359, pp. 177–190.

Fisher, J.A., Nichols, G.J., Waltham, D.A., 2007. Unconfined flow deposits in distal sectors of fluvial distributary systems: examples from the Miocene Luna and Huesca Systems, northern Spain. Sedimentary Geology 195, 55–73.

Gibert, L., Sanz de Galdeano, C., Alfaro, P., Scott, G., López Garrido, A.C., 2005. Seismic-induced slump in Early Pleistocene deltaic deposits of the Baza Basin (SE Spain). Sedimentary Geology 179, 279–294.

Harshbarger, J.W., Repenning, C.A., Irwin, J.H., 1957. Stratigraphy of the uppermost Triassic and the Jurassic rocks of the Navajo Country. U.S. Geological Survey Professional Paper 291, 12–26.

Hesse, R., Reading, H.G., 1978. Subaqueous clastic fissure eruption and other examples of sedimentary transposition in the lacustrine Horton Bluff Formation (Mississippian), Nova Scotia. Canadian Specialist Publications International Associations of Sedimentologists 2, 241–257.

Irby, G.V., 1996a. Synopsis of the Moenave Formation. In: Morales, M. (Ed.), Guidebook for the Geological Excursion of the Continental Jurassic Symposium. Museum of Northern Arizona, Flagstaff, pp. 3–14.

Irby, G.V., 1996b. Paleoichnology of the Cameron dinosaur tracksite, Lower Jurassic Moenave Formation, northeastern Arizona. In: Morales, M. (Ed.), The Continental Jurassic: Museum of Northern Arizona Bulletin, vol. 60, pp. 147–166.

Johnston, A.C., Schweig, E.S., 1996. The enigma of the New Madrid earthquakes of 1811–1812. Annual Review of Earth and Planetary Sciences 24, 39–384.

Jones, A.P., Omoto, K., 2000. Towards establishing criteria for identifying trigger mechanisms for soft-sediment deformation: a case study of Late Pleistocene lacustrine sands and clays, Onkobe and Nakayamadaira Basins, northeastern Japan. Sedimentology 47, 1211–1226.

Kent, D.V., Olsen, P.E., 1997. Magnetostratigraphy and paleopoles from the Late Triassic Dan River–Danville basin: interbasin correlation of continental sediments and a test of the tectonic coherence of the Newark rift basins in eastern North America. Geological Society of America Bulletin 109, 366–379.

Kirkland, J.I., Milner, A.R.C., 2006. The Moenave Formation at the St. George Dinosaur Discovery Site at Johnson Farm. New Mexico Museum of Natural History and Science Bulletin 37, 289–309.

Koç Taşgın, C., Türkmen, I., 2009. Analysis of soft-sediment deformation structures in Neogene fluvio-lacustrine deposits of Çaybağı Formation, Eastern Turkey. Sedimentary Geology 218, 16–30.

Last, W.M., Deleqiat, J., Greengrass, K., Sukhan, S., 2002. Re-examination of the recent history of meromictic Waldesa Lake, Saskatchewan, Canada. In: Tiercelin, J.-J. (Ed.), Lacustrine Depositional Systems: Sedimentary Geology, vol. 148, pp. 147–160.

Litwin, R.J., 1986. The palynostratigraphy and age of the Chinle and Moenave formations, southwestern USA [Ph.D. dissertation]. The Pennsylvania State University, College Park, 265 pp.

Lowe, D.R., 1975. Water escape structures in coarse-grained sediments. Sedimentology 22, 157–204.

Lowe, D.R., LoPiccolo, R.D., 1974. The characteristics and origins of dish and pillar structures. Journal of Sedimentary Petrology 44, 484–501.

Lucas, S.G., 1993. The Chinle Group: revised stratigraphy and chronology of Upper Triassic nonmarine strata in the western United States. Museum of Northern Arizona Bulletin 59, 27–50.

Lucas, S.G., Heckert, A.B., 2001. Theropod dinosaurs and the Early Jurassic age of the Moenave Formation, Arizona–Utah, USA. Neues Jahrbuch fuer Geologie und Palaeontologie, Monatshefte 7, 435–448.

Lucas, S.G., Tanner, L.H., 2006. The Springdale Member of the Kayenta Formation, Lower Jurassic of Utah–Arizona. New Mexico Museum of Natural History and Science Bulletin 37, 71–76.

Lucas, S.G., Tanner, L.H., 2007. Tetrapod biostratigraphy and biochronology of the Triassic–Jurassic transition on the southern Colorado Plateau, USA. Palaeogeography, Palaeoclimatology, Palaeoecology 244, 242–256.

Lucas, S.G., Heckert, A.B., Estep, J.W., Anderson, O.J., 1997. Stratigraphy of the Upper Triassic Chinle Group, Four Corners region. Mesozoic Geology and Paleontology of the Four Corners Region: New Mexico Geological Society Guidebook, vol. 48, pp. 81–108.

Lucas, S.G., Tanner, L.H., Heckert, A.B., 2005. Tetrapod biostratigraphy and biochronology across the Triassic–Jurassic boundary in northeastern Arizona. New Mexico Museum of Natural History and Science Bulletin 29, 84–94.

Maltman, A., 1994. Introduction and overview. In: Maltman, A. (Ed.), The Geological Deformation of Sediments. Chapman and Hall, London, pp. 1–35.

Maltman, A., Bolton, A., 2003. In: Van Rensbergen, P., Maltman, R.R., Morley, C.K. (Eds.), How sediments become mobilized. Subsurface Sediment Mobilization, vol. 216. Geological Society Special Publication, London, pp. 9–20.

Mariotti, G., Corda, L., Brandano, M., Civitelli, G., 2002. Indicators of paleoseismicity in the lower to middle Miocene Guadagnolo Formation, central Apennines, Italy. In: Ettensohn, F.R., Rast, N., Brett, C.E. (Eds.), Ancient Seismites: Geological Society of America Special Paper, vol. 359, pp. 87–97.

Marzolf, J.E., 1993. Palinspastic reconstruction of early Mesozoic sedimentary basins near the latitude of Las Vegas; implications for the early Mesozoic Cordilleran cratonal margin. In: Dunne, G.C., McDougal, K.A. (Eds.), Mesozoic Paleogeography of the Western United States: Field Trip Guidebook – Pacific Section SEPM, vol. 71, pp. 433–462.

Marzolf, J.E., 1994. Reconstruction of the early Mesozoic Cordilleran cratonic margin adjacent to the Colorado Plateau. In: Caputo, M.V., Peterson, J.A., Franczyk, K.J. (Eds.), Mesozoic Systems of the Rocky Mountain Region, USA. Rocky Mountain Section SEPM, Denver, pp. 181–215.

McGlaughlin, P.I., Brett, C.E., 2004. Eustatic and tectonic control on the distribution of marine seismites: examples from the Upper Ordovician of Kentucky, USA. Sedimentary Geology 168, 165–192.

Merriam, D.F., Förster, A., 2002. Stratigraphic and sedimentologic evidence for late Paleozoic earthquakes and recurrent structural movement in the U.S. Midcontinent. In: Ettensohn, F.R., Rast, N., Brett, C.E. (Eds.), Ancient Seismites: Geological Society of America Special Paper, vol. 359, pp. 99–107.

Mills, P.C., 1983. Genesis and diagnostic value of soft-sediment deformation structures — a review. Sedimentary Geology 35, 83–104.

Milner, A.R.C., Kirkland, J.I., 2006. Preliminary review of the Early Jurassic (Hettangian) freshwater Lake Dixie fish fauna in the Whitmore Point Member, Moenave Formation in southwest Utah. New Mexico Museum of Natural History and Science Bulletin 37, 510–521.

Molina-Garza, R.S., Geissman, J.W., Van der Voo, R., 1995. Paleomagnetism of the Dockum Group (Upper Triassic), northwest Texas: further evidence for the J-1 cusp in the North American apparent polar wander path and implications for the apparent polar wander and Colorado Plateau migration. Tectonics 14, 979–993.

Molina-Garza, R.S., Geissman, J.W., Lucas, S.G., 2003. Paleomagnetism and magnetostratigraphy of the lower Glen Canyon and upper Chinle Groups, Jurassic–Triassic of northern Arizona and northeast Utah. Journal of Geophysical Research 108 (B4), 2181. doi:10.1029/2002JB001909.

Morales, M., 1996. Brief report on theropod trackways in the Wingate Sandstone of Ward Terrace, Arizona. In: Morales, M. (Ed.), The Continental Jurassic: Museum of Northern Arizona Bulletin, vol. 60, pp. 169–171.

Moretti, M., Sabato, L., 2007. Recognition of trigger mechanisms for soft-sediment deformation in the Pleistocene lacustrine deposits of the Sant 'Arcangelo Basin (Southern Italy): seismic shock vs. overloading. Sedimentary Geology 196, 31–45.

Moretti, M., Pieri, P., Tropeano, M., 2002. Late Pleistocene soft-sediment deformation structures interpreted as seismites in paralic deposits in the city of Bari (Apulian foreland, southern Italy). In: Ettensohn, F.R., Rast, N., Brett, C.E. (Eds.), Ancient Seismites: Geological Society of America Special Paper, vol. 359, pp. 75–85.

Neuwerth, R., Suter, F., Guzman, C.A., Gorin, G.E., 2006. Soft-sediment deformation in a tectonically active area: the Plio-Pleistocene Zarzal Formation in the Cauca Valley (Western Colombia). Sedimentary Geology 186, 67–88.

Nichols, G.J., Fisher, J.A., 2007. Processes, facies and architecture of fluvial distributary system deposits. Sedimentary Geology 195, 75–90.

Obermeier, S.F., 1996. Use of liquefaction-induced features for paleoseismic analysis — an overview of how seismic liquefaction features can be distinguished from other features and how their regional distribution and properties of source sediment can be used to infer the location and strength of Holocene paleo-earthquakes. Engineering Geology 44, 1–76.

Obermeier, S.F., 1998. Liquefaction evidence for strong earthquakes of Holocene and latest Pleistocene ages in the states of Indiana and Illinois, USA. Engineering Geology 50, 227–254.

Obermeier, S.F., Jacobson, R.B., Smoot, J.P., Weems, R.E., Gohion, G.S., Monroe, J.E., Powars, D.S., 1990. Earthquake-induced liquefaction features in the coastal setting of South Carolina and in the fluvial setting of the New Madrid seismic zone. United States Geological Survey Professional Paper 1504, 44 pp.

Oliveira, C.M., Hodgson, D.M., Flint, S.S., 2009. Aseismic controls on in situ soft-sediment deformation processes and products in submarine slope deposits of the Karoo Basin, South Africa. Sedimentology 56, 1201–1225.

Olsen, H., 1989. Sandstone-body structures and ephemeral stream processes in the Dinosaur Canyon Member, Moenave Formation (Lower Jurassic), Utah, U.S.A. Sedimentary Geology 61, 207–221.

Owen, G., 1987. Deformation processes in unconsolidated sands. In: Jones, M.E., Preston, R.M.F. (Eds.), Deformation of Sediments and Sedimentary Rocks: Geological Society (London) Special Publication, vol. 29, pp. 11–24.

Owen, G., 1996. Experimental soft-sediment deformation: structures formed by the liquefaction of unconsolidated sands and some ancient examples. Sedimentology 43, 279–293.

Owen, G., 2003. Load structures: gravity-driven sediment mobilization in the shallow subsurface. In: Van Rensebergen, P., Hillis, R.R., Maltman, A.J., Morley, C.K. (Eds.), Subsurface Sediment Mobilization: Geological Society (London) Special Publication, vol. 216, pp. 21–34.

Parrish, J.T., 1993. Climate of the supercontinent Pangea. Journal of Geology 101, 215–253.

Peterson, F., Pipiringos, G.N., 1979. Stratigraphic relations of the Navajo Sandstone to Middle Jurassic formations, southern Utah and northern Arizona. U.S. Geological Survey Professional Paper 1035-B.

Pietras, J.T., Carroll, A.R., 2006. High resolution stratigraphy of an underfilled lake basin; Wilkins Peak member, Eocene Green River Formation, Wyoming, U.S.A. Journal of Sedimentary Research 76, 1197–1214.

Pipiringos, G.N., O'Sullivan, R.N., 1978. Principal unconformities in Triassic and Jurassic rocks, western interior United States — a preliminary survey. United States Geological Survey Professional Paper 1035-A, 1–29.

Plint, A.G., 1985. Possible earthquake-induced soft-sediment faulting and remobilization in Pennsylvanian alluvial strata, southern New Brunswick, Canada. Canadian Journal of Earth Science 22, 907–912.

Pope, M.C., Read, J.F., Bambach, R.K., Hofmann, H.J., 1997. Late Middle to Late Ordovician seismites of Kentucky, southwest Ohio and Virginia: sedimentary recorders of earthquakes in the Appalachian basin. Geological Society of America Bulletin 109, 489–503.

Potter, P.W., Pettijohn, F.J., 1963. Paleocurrents and Basin Analysis. Academic Press Inc., New York. 296 pp.

Rodrìguez Pascua, M.A., Calvo, J.P., De Vicente, G., Gomez Gras, D., 2000. Seismites in lacustrine sediments of the Prebetic Zone, SE Spain, and their use as indicators of earthquake magnitudes during the Late Miocene. Sedimentary Geology 135, 117–135.

Rossetti, D.F., 1999. Soft-sediment deformation structures in late Albian to Cenomanian deposits, Sao Luis Basin, northern Brazil: evidence for palaeoseismicity. Sedimentology 46, 1065–1081.

Rossetti, D.F., Góes, A.M., 2000. Deciphering the sedimentological imprint of paleoseismic events: an example from the Aptian Codó Formation, northern Brazil. Sedimentary Geology 135, 137–156.

Scotese, C.R., 1994. Late Triassic paleogeographic map. In: Klein, G.D. (Ed.), Pangea: Paleoclimate, Tectonics, and Sedimentation During Accretion, Zenith, and Breakup of a Supercontinent: Geological Society of America Special Paper, vol. 288, p. 7.

Scott, B., Price, S., 1988. Earthquake-induced structure in young sediments. Tectonophysics 147, 165–170.

Seilacher, A., 1969. Fault-graded beds interpreted as seismites. Sedimentology 13, 155–159.

Seilacher, A., 1984. Sedimentary structures tentatively attributed to seismic events. Marine Geology 55, 1–12.

Selker, J.S., 1993. Expressions for the formation of load casts in soft sediment. Journal of Sedimentary Petrology 63, 1149–1151.

Sims, J.D., 1973. Earthquake-induced structures in sediments of Van Norman Lake, San Fernando, California. Science 182, 161–163.

Sims, J.D., 1975. Determining earthquake recurrence intervals from deformational structures in young lacustrine sediments. Tectonophysics 29, 141–152.

Singh, S., Jain, A.K., 2007. Liquefaction and fluidization of lacustrine deposits from Lahaul-Spiti and Ladakh Himalaya: geological evidences of paleoseismicity along active fault zone. Sedimentary Geology 196, 47–57.

Smoot, J.P., Lowenstein, T.K., 1991. Depositional environments of non-marine evaporites. In: Melvin, J.L. (Ed.), Evaporites, Petroleum and Mineral Resources. Developments in Sedimentology, vol. 50. Elsevier, New York, pp. 189–347.

Sneh, A., 1983. Desert stream sequences in the Sinai Peninsula. Journal of Sedimentary Petrology 53, 2171–2180.

Stanley, K.O., Surdam, R.C., 1978. Sedimentation on the front of Eocene Gilbert-type deltas, Washakie Basin, Wyoming. Journal of Sedimentary Petrology 48, 557–573.

Talbot, M.R., Holm, K., Williams, M.A.J., 1994. Sedimentation in low gradient desert margin systems; a comparison of the Late Triassic of northwest Sommerset (England) and the Late Quaternary of east-central Australia. In: Rosen, M.R. (Ed.), Palaeoclimate and Basin Evolution of Playa Systems: Geological Society of America Special Paper, vol. 289, pp. 97–117.

Talwani, P., Cox, J., 1985. Paleoseismic evidence for recurrence of earthquakes near Charleston, South Carolina. Science 229, 379–381.

Tanner, L.H., 2000. Palustrine–lacustrine and alluvial facies of the (Norian) Owl Rock Formation (Chinle Group), Four Corners Region, southwestern U.S.A.: implications for Late Triassic paleoclimate. Journal of Sedimentary Research 70, 1280–1289.

Tanner, L.H., 2003a. Possible tectonic controls on Late Triassic sedimentation in the Chinle basin, Colorado Plateau. New Mexico Geologic Society Guidebook, 54th Field Conference, pp. 261–267.

Tanner, L.H., 2003b. Pedogenic record of paleoclimate and basin evolution in the Triassic–Jurassic Fundy rift basin, eastern Canada. In: LeTourneau, P.M., Olsen, P.E. (Eds.), The Great Rift Valleys of Pangea in Eastern North America. Columbia University Press, New York, pp. 108–122.

Tanner, L.H., Lucas, S.G., 2007. The Moenave Formation: sedimentologic and stratigraphic context of the Triassic–Jurassic boundary in the Four Corners area, southwestern U.S.A. Palaeogeography, Palaeoecology, Palaeoclimatology 244, 111–125.

Tanner, L.H., Lucas, S.G., 2009. The Whitmore Point Member of the Moenave Formation: Early Jurassic dryland lakes on the Colorado Plateau, Southwestern USA. Volumina Jurassica 6, 11–21.

Tooth, S., 2000. Downstream changes in dryland river channels: the northern plains of arid central Australia. Geomorphology 34, 33–54.

Tunbridge, I.P., 1981. Sandy high-energy flood sedimentation — some criteria for recognition, with an example from the Devonian of S.W. England. Sedimentary Geology 28, 79–95.

Turcq, B., Albuquerque, A.L.S., Cordeiro, R.C., Sifeddine, A., Simoes Filho, F.F.L., Souza, A.G., Abrao, J.J., Oliveira, F.B.L., Silva, A.O., Capitaneo, J., 2002. Accumulation of organic carbon in five Brazilian lakes during the Holocene. In: Tiercelin, J.-J. (Ed.), Lacustrine Depositional Systems: Sedimentary Geology, vol. 148, pp. 319–342.

Van Loon, A.J., Brodzikowski, K., Zielinski, 1995. Shock-induced resuspension deposits from a Pleistocene proglacial lake (Kleszców Graben, central Poland). Journal of Sedimentary Research A65 (2), 417–422.

Vittori, E., Labini, S.S., Serva, L., 1991. Palaeoseismology; review of the state-of-the-art. Tectonophysics 193, 9–32.

Wheeler, R.L., 2002. Distinguishing seismic from nonseismic soft-sediment structures: criteria from seismic-hazard analysis. In: Ettensohn, F.R., Rast, N., Brett, C.E. (Eds.), Ancient Seismites: Geological Society of America Special Paper, vol. 359, pp. 1–11.

Wilson, R.F., 1967. Whitmore Point, a new member of the Moenave Formation in Utah and Arizona. Plateau 40, 29–40.